Achieving Extreme Light Confinement in Low-Index-Dielectric Resonators Through Quasi-Bound States in the Continuum

WEI WANG[1,2] AND XUEDAN MA[1,2,3*]

[1] Center for Nanoscale Materials, Argonne National Laboratory, Lemont, Illinois 60439, United States
[2] Consortium for Advanced Science and Engineering, University of Chicago, Chicago, Illinois 60637, United States
[3] Northwestern-Argonne Institute of Science and Engineering, Northwestern University, 2205 Tech Drive, Evanston, IL 60208, USA
[*] Corresponding author: xuedan.ma@anl.gov

Compiled November 3, 2021

Obtaining large field enhancement in low-refractive-index dielectric materials is highly relevant to many photonic and quantum optics applications. However, confining light in these materials is challenging due to light leakage through coupling to continuum modes in the surrounding environment. We investigate the possibility of achieving high quality factors in low-index dielectric resonators through the bound states in the continuum (BIC). Our simulations demonstrate that destructive interference between leaky modes can be achieved by tuning the geometrical parameters of the resonator arrays, which leads to the emergence of quasi-BIC in resonators that have a small index contrast to the underlying substrates. The resultant large field enhancement gives rise to giant quality factors and Purcell effects. By introducing vertical mirror symmetry, the quasi-BIC can be tuned into an ideal BIC. Additionally, the quasi-BIC can modify the emission patterns of the coupled emitters, rendering highly directional and focused far-field emission. These findings may provide a path for the practical implementation of photonic and quantum devices based on low-index dielectric materials.

http://dx.doi.org/10.1364/ao.XX.XXXXXX

Dielectric resonators that possess a rich family of resonance modes[1, 2] can support many intriguing effects such as the Kerker effect that suppresses backward scattering[3] and highly efficient harmonic generation enabled by anapole mode excitation.[4] The low dissipative losses of the dielectric resonators offer unique opportunities for subwavelength light trapping. The achievement of high quality factors (Q) and large resonant enhancement of the electric and magnetic near-fields in the dielectric resonators [5, 6] are of particular interest for nanophotonics and quantum optics applications.[7, 8]

Despite these appealing properties offered by the dielectric resonators, only those with sufficiently high refractive indices are known to support well-defined resonance modes.[1, 9] This poses severe limitations on the effective usage of the dielectric resonators. Particularly, the resonance modes in the dielectric resonators are typically confined inside the resonators. In order to maximize the spatial overlap between the dielectric resonance modes and external gain media, direct integration of the gain media into the resonators is required. However, this often diminishes the resonance modes in the high-index resonators and lowers their quality factors.[7] In this regard, a strategy for achieving large field enhancement and quality factors in low-refractive-index dielectric materials such as polymers, oxides and semiconductors that would allow the direct integration of gain media to the dielectric resonance modes[10–12] is particularly desirable. Current efforts in this direction have relied on approaches such as using index contrast between the dielectric resonators and their surrounding environment,[13, 14] and only moderate field enhancement has been achieved.

Originally proposed in quantum mechanics, bound states in the continuum (BIC) formed through destructive interference between two or more leaky modes or resonators have been widely used for light trapping and guiding.[15, 16] The realization of optical BIC in subwavelength dielectric resonators with high refractive indices could lead to quality factors comparable to those of the extensively studied photonic cavities such as photonic crystals.[5, 17] However, due to the difficulty in confining resonance modes in low-refractive-index dielectric resonators, studies on BIC in these resonators remain sparse despite their high relevance to enhanced light-matter interactions.

Here, we discuss the realization of BIC in low-refractive-index dielectric resonators through numerical simulations. Due to destructive interference between propagating modes supported by the resonator arrays and localized modes in the resonators, quasi-BIC supporting large quality factors can be observed in dielectric resonators with refractive indices close to the underlying substrates. The well confined field enabled by the quasi-BIC results in giant Purcell factors. Moreover, it also leads to highly focused and directional far-field emission. Additionally, we find that when vertical mirror symmetry is introduced to the structure by covering the resonator arrays with dielectric layers of the same refractive indices as the underlying substrates, the quasi-BIC can transition into ideal BIC. These findings could open new

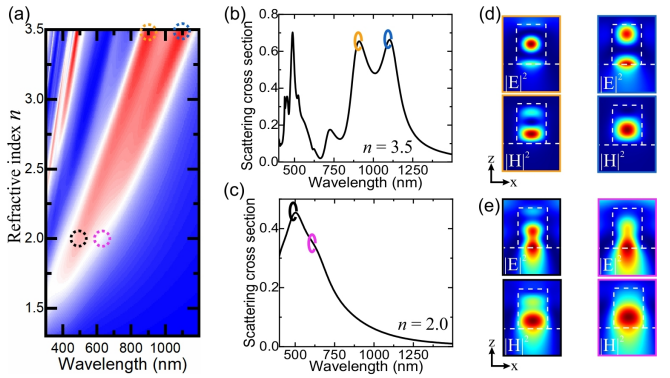

Fig. 1. (a) Reflectance spectra of a dielectric cylinder with a diameter of 250 nm and height of 330 nm placed on a silica substrate. The color-coded circles correspond to the highlighted resonance modes in (b) and (c). (b) and (c) The reflectance spectra of a dielectric cylinder with n = 3.5 (b) and 2.0 (c). (d) and (e) The electric and magnetic field intensity distributions at the resonance wavelengths shown in (b) and (c).

perspectives for the application of BIC in nanophotonics and quantum optics.

Light in low-refractive-index dielectric structures typically undergoes radiation loss through coupling to continuum modes in the substrates or embedding materials. To clearly demonstrate this concept, we start by simulating a dielectric cylinder with various refractive indices placed on a silica substrate (see Supplement S1 for the detailed simulation method).

As shown in **Figure 1**, a change in the refractive index of the dielectric resonator not only affects its resonance wavelengths, but also the field distributions of the supported modes. At n = 3.5 (Figure 1b and 1d), two distinct resonance modes can be clearly resolved with the one at 900 nm exhibiting electric dipole characteristics and the one at 1100 nm magnetic dipole characteristics (see Supplement S2 for field distributions in horizontal planes). Both resonance modes are well confined inside the dielectric resonator. When the refractive index of the resonator is reduced to n = 2.0, the resonance modes are no longer well defined aside from the apparent reduction in the scattering cross section, as shown in Figure 1c. Moreover, instead of being well confined in the dielectric resonator, a significant part of the electromagnetic fields have leaked into the underlying substrate (Figure 1e). Evidently, radiation loss through the continuum modes in the substrates becomes more severe in dielectric resonators with low refractive indices.

BIC offers an appealing approach for achieving high quality optical resonance modes even in the existence of continuum radiation channels that would normally carry away the energies. Of the different types of structures proposed for achieving BIC, using destructive interference between two leaky modes enabled by combining several subwavelength resonators gives the degree of freedom to tune the achievable quality factors and resonance frequencies.[15] We consider a 2D infinite periodic array of dielectric cylinders with diameter D, height H, edge-to-edge gap G, and pitch P placed on silica substrates, as shown in the inset of **Figure 2a**. As an illustrative case, the refractive index of the dielectric cylinders is set to be 1.8, a value representative of many low-index dielectric materials such as alumina, indium tin oxide and hexagonal boron nitride (hBN), that are of high relevance to many photonic applications and allow the direct

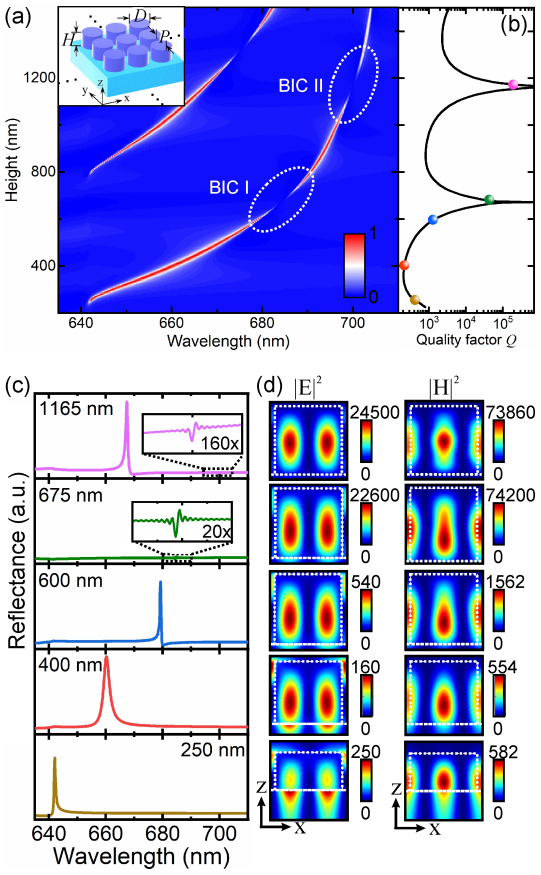

Fig. 2. (a) Height-dependent reflectance spectra of an infinite periodic array of dielectric cylinders with diameter D = 390 nm, pitch P = 440 nm and refractive index n = 1.8 placed on a silica substrate. Inset: layout of the considered array structure. (b) The corresponding height-dependent quality factors Q. (c) Reflectance spectra of the dielectric resonator arrays with the indicated heights. The color codes correspond to the dots highlighted in (b). The vertical range of the spectra are normalized to the same scale. (d) Local electric and magnetic field intensity distributions at the corresponding heights. The fields are normalized to those in the absence of the resonator arrays.

integration of emitters.[11, 18] To alter the resonance conditions of the structures, the height H of the resonators is tuned while all other parameters are kept constant. As shown in Figure 2a and Figure 2c bottom, at the height H = 250 nm, a sharp, Fano-like resonance peak can be observed at the wavelength of around 640 nm. This resonance mode can be attributed to the so-called Rayleigh anomaly,[19] an effect induced by the interference between the guided resonance modes supported by the periodic structures and the directly reflected light. The electromagnetic field distributions exhibit clear magnetic dipole characteristics (Figure 2d, bottom). Due to the larger impedance mismatch towards the substrate, a high leaky condition can be observed and the magnetic dipole mode is attracted towards the lower part of the resonator. A careful inspection of the reflectance spectral characteristics by fitting it with the classical Fano formula[20] reveals a quality factor on the order of 10^3 (Figure 2b, right).

With an increase in the resonator height, the reflectance spectrum red shifts and gains more symmetry due to the vanishing effect of the Rayleight anomaly (Figure 2c, red curve) and con-

sequently, the quality factor reduces slightly (Figure 2b). As the height of the dielectric resonators further increases and approaches 675 nm, the reflectance spectrum becomes sharper and turns into highly asymmetric Fano lineshape, accompanied by a drastic reduction in the reflectance amplitude. The resonance peak eventually gets close to a minimum value, as indicated by the dashed circle in Figure 2a, as well as the reflectance spectrum in Figure 2c (green curve). The quality factor of the resonance mode obtained by fitting the resonance peak with Fano formula increases correspondingly. Additionally, the field enhancement inside the dielectric resonators increases drastically (Figure 2d). Our calculations of the wave-vector resolved quality factor for H = 675 nm also yields a maximum value at the Brillouin zone center (Supplement S3). These features are characteristic of quasi-BIC. Ideal BIC is completely decoupled from the continuum and supports infinite quality factors, but it can only exist in lossless infinite structures or in finite structures composed of materials with zero or infinite permittivity.[16] Once the conditions are slightly detuned from the ideal BIC condition, the BIC mode manifests itself as a Fano resonance lineshape due to the interference of the modes.[15, 16] We refer to the quasi-BIC mode at the resonance wavelength of around 685 nm as the quasi-BIC I mode. A second quasi-BIC region (quasi-BIC II) can be observed at the wavelength of around 700 nm, at which a maximum quality factor can be observed again.

Notably, the quasi-BIC modes demonstrated here are trapped in the resonators and have vanishing field distributions in the substrates (Figure 2d and Supplement S4). It can be affected by geometrical parameters rather than incident light direction. Aside from the resonator height as shown in Figure 2a, tuning the resonator diameter and the gap between the resonators (see Supplement S5) can also result in reduced quality factors.[5] Dissipative losses can smear out the quasi-BIC (Supplement S5), although the application of low-loss materials such as optical glasses and polymers or the utilization of gain can circumvent this problem.[21] Interestingly, we discover that ideal BIC can be achieved in the low-index resonator arrays if we introduce mirror symmetry in the vertical direction by embedding the resonators in uniform dielectric environments (see Supplement S3 for details).

Quasi-BIC in such dielectric resonator arrays can be observed even for materials with a refractive index as small as 1.6 (Supplement S6), which is close to that of the underlying silica substrates. We note though as the refractive indices of the dielectric resonators approach these of the substrates, the nonzero reflection from the substrates and the weak reflection from the resonators make it challenging to resolve the quasi-BIC modes.

The drastic enhancement in the electromagnetic fields inside the dielectric resonators provides the possibility to utilize them for enhanced emission. We evaluate the Purcell factor of the quasi-BIC mode shown in Figure 2a (green dot). Due to the magnetic dipole nature of the resonance modes supported by the dielectric resonators, we focus on their coupling to an emitter possessing a magnetic dipole moment, although similar analysis also applies to emitters with electric dipole moments. For the dielectric resonator arrays with conditions shown in Figure 2(a) (green dot), a maximum Purcell factor (P_F) of around 7.9×10^3 can be achieved for a magnetic dipole moment that is resonant with the array resonance wavelength and also positioned and oriented with respect to the local magnetic fields.

So far, in order to identify the BIC conditions, we have considered the resonator arrays to be infinite in size, which is difficult to achieve in practice. To gain a more thorough understanding

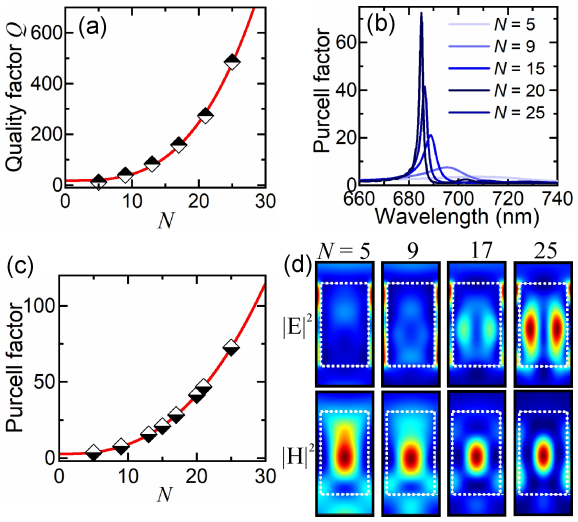

Fig. 3. (a) Array size N-dependent quality factors Q of the dielectric resonator array with H = 675 nm, P = 440 nm, D = 390 nm and refractive index n = 1.8. The curve is an allometric growth fit to the data points. (b) Wavelength-dependent Purcell factors of the resonator array with different array sizes. (c) Array size N-dependent Purcell factors of the dielectric resonator array at the resonance wavelengths. The curve is an allometric growth fit to the data points. (d) Local electric and magnetic field intensity distributions of the dielectric resonator array with various array sizes. The geometrical parameters of the resonators in (b) - (d) are the same as those in (a).

of the quasi-BIC discussed here and the properties of experimentally achievable quasi-BIC conditions, we study the influence of the resonator array size N. **Figure 3a** shows the array size-dependent quality factors of dielectric resonator arrays with their geometrical parameters tuned to be the same as those shown in Figure 2a (green dot). With an increase in the array size, the quality factor also increases and it exhibits N-dependent growth behavior: $Q \propto N^{3.2}$. The calculation of the corresponding maximum Purcell factors for resonant magnetic dipole moments that are coupled to the dielectric resonators also indicate a strong N-dependency: $P_F \propto N^{2.6}$ (Figure 3b and 3c). The approximate N^3 growth rates of the quality factors and Purcell factors are likely related to the Bloch wave dispersion of the array structures near the band edge,[22] which has been observed in other systems possessing similar dispersion curves.[23] A careful inspection of the local field distributions help reveal the formation of quasi-BIC in the dielectric resonators. As shown in Figure 3d, when the array size N is small, a significant portion of the field is lost through coupling to the surrounding environment, as is expected for low-index dielectric resonators. However, when N increases, the increasing destructive interference between the evanescent fields leaking from the resonator local modes and the propagating modes supported by the resonator arrays inhibits the coupling of the resonators to continuum, resulting in highly confined fields inside the low-index resonators.

The influence of the array size on the quasi-BIC mode is not only reflected in the field enhancement inside the resonators, but also the radiation patterns of the dipole moments coupled to the field. **Figure 4a** and 4b show the emission patterns of a magnetic dipole moment coupled to an array of the dielectric resonators. Due to the periodic 2D square array layout of the resonators, the emission of the dipole moment is highly symmetric and

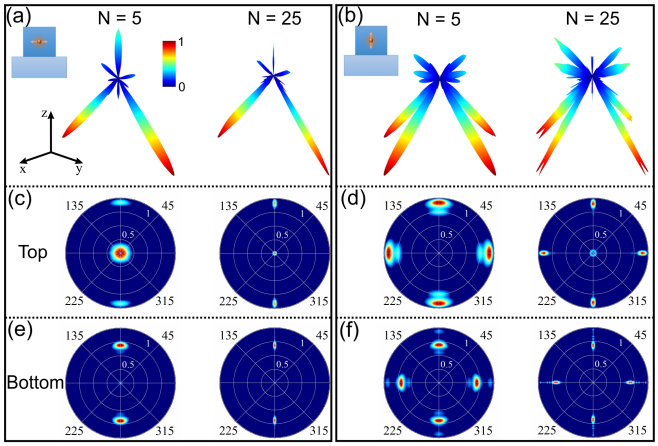

Fig. 4. (a) Radiation patterns of a magnetic dipole moment lying horizontally in a dielectric resonator array with the size of $N = 5$ (left) and 25 (right). The resonator array has $H = 675$ nm, $P = 440$ nm, $D = 390$ nm and refractive index $n = 1.8$. (b) Radiation patterns of a magnetic dipole moment lying vertically in a dielectric resonator array with the size of $N = 5$ (left) and 25 (right). The parameters of the resonator array is the same as those in (a). (c, e) Far-field projections of emission from the structure in (a) viewed from top (c) and bottom (e) of the structure. (d, f) Far-field projections of emission from the structure in (b) viewed from top (d) and bottom (f) of the structure.

mainly directed towards the substrates (termed as forward). For a horizontally lying magnetic dipole moment, its emission is predominantly composed of two lobes directed at an angle of 64 degree forward and a much weaker lobe pointing straight backward. This is further illustrated by the far-field emission patterns shown in Figure 4c and 4e. In the case of a vertically lying dipole, its emission pattern exhibits a 4-fold symmetry with 4 lobes pointing at an angle of 64 degree forward and another 4 backward (Figure 4b, 4d and 4f). As the array size N increases, the symmetry of the emission patterns remain the same, although the far-field emission spots become notably more focused. The highly focused, directional emission observed here can significantly improve light collection efficiencies that would be beneficial for lasing and quantum photon sources.[24]

In summary, we study the formation of quasi-BIC in low-index dielectric resonator arrays and their coupling to emissive dipoles. The giant quality factors enabled by the quasi-BIC modes, combined with the flexibility of the low-index dielectric resonators that would allow the direct integration of gain materials without compromising the quasi-BIC modes, could lead to immense Purcell factors that are essential for many photonic applications. We also investigate the influence of the resonator array size on the formation of quasi-BIC and observe an approximate N^3 growth rate for both the quality factors and Purcell factors. Our simulations of emission dipole moments coupled to the resonator arrays show that their far-field emission patterns are highly directional and focused. These findings may open a new avenue for the practical application of low-index dielectric resonators in quantum photonics.

Acknowledgments. This work was performed, in part, at the Center for Nanoscale Materials, a U.S. Department of Energy Office of Science User Facility, and supported by the U.S. Department of Energy, Office of Science, under Contract No. DE-AC02-06CH11357. X.M. acknowledges support from the National Science Foundation CBET Program under the award no. 2025214.

Disclosures. The authors declare no conflicts of interest.

Data Availability Statement. Data underlying the results presented in this paper are not publicly available at this time but may be obtained from the authors upon reasonable request.

Supplemental document. See Supplement for supporting content.

REFERENCES

1. A. I. Kuznetsov, A. E. Miroshnichenko, M. L. Brongersma, Y. S. Kivshar, and B. Luk'yanchuk, Science **354**, aag2472 (2016).
2. A. B. Evlyukhin, C. Reinhardt, A. Seidel, B. S. Luk'yanchuk, and B. N. Chichkov, Phys. Rev. B **82**, 045404 (2010).
3. V. E. Babicheva and A. B. Evlyukhin, Laser Photonics Rev. **11**, 1700132 (2017).
4. G. Grinblat, Y. Li, M. P. Nielsen, R. F. Oulton, and S. A. Maier, Nano Lett. **16**, 4635 (2016).
5. M. V. Rybin, K. L. Koshelev, Z. F. Sadrieva, K. B. Samusev, A. A. Bogdanov, M. F. Limonov, and Y. S. Kivshar, Phys. Rev. Lett. **119**, 243901 (2017).
6. K. Koshelev, S. Kruk, E. Melik-Gaykazyan, J.-H. Choi, A. Bogdanov, H.-G. Park, and Y. Kivshar, Science **367**, 288 (2020).
7. V. Rutckaia, F. Heyroth, A. Novikov, M. Shaleev, M. Petrov, and J. Schilling, Nano Lett. **17**, 6886 (2017).
8. X. Ma, A. R. James, N. F. Hartmann, J. K. Baldwin, J. Dominguez, M. B. Sinclair, T. S. Luk, O. Wolf, S. Liu, S. K. Doorn, H. Htoon, and I. Brener, ACS Nano **11**, 6431 (2017).
9. A. García-Etxarri, R. Gómez-Medina, L. S. Froufe-Pérez, C. López, L. Chantada, F. Scheffold, J. Aizpurua, M. Nieto-Vesperinas, and J. J. Sáenz, Opt. Exp. **19**, 4815 (2011).
10. H. Qiao, B. Guan, T. Böcking, M. Gal, J. J. Gooding, and P. J. Reece, Appl. Phys. Lett. **96**, 161106 (2010).
11. S. Kim, J. E. Fröch, J. Christian, M. Straw, J. Bishop, D. Totonjian, K. Watanabe, T. Taniguchi, M. Toth, and I. Aharonovich, Nat. Commun. **9**, 2623 (2018).
12. X. Ma, N. F. Hartmann, J. K. S. Baldwin, S. K. Doorn, and H. Htoon, Nat. Nanotechnol. **10**, 671 (2015).
13. K.-H. Kim and W.-S. Rim, ACS Photon. **5**, 4769 (2018).
14. J. Zhou, A. Panday, Y. Xu, X. Chen, L. Chen, C. Ji, and L. J. Guo, Phys. Rev. Lett. **120**, 253902 (2018).
15. C. W. Hsu, B. Zhen, A. D. Stone, J. D. Joannopoulos, and M. Soljačić, Nat. Rev. Mater. **1**, 16048 (2016).
16. F. Monticone, H. M. Doeleman, W. D. Hollander, A. F. Koenderink, and A. Alù, Laser Photonics Rev. **12**, 1700220 (2018).
17. S. T. Ha, Y. H. Fu, N. K. Emani, Z. Pan, R. M. Bakker, R. Paniagua-Domínguez, and A. I. Kuznetsov, Nat. Nanotechnol. **13**, 1042 (2018).
18. S. Ayas, A. E. Topal, A. Cupallari, H. Guner, G. Bakan, and A. Dana, ACS Photonics **1**, 1313 (2014).
19. Y. Shen, V. Rinnerbauer, I. Wang, V. Stelmakh, J. D. Joannopoulos, and M. Soljačić, ACS Photon. **2**, 24 (2015).
20. C. S. Kim, A. M. Satanin, Y. S. Joe, and R. M. Cosby, Phys. Rev. B **60**, 10962 (1999).
21. F. Todisco, M. Esposito, S. Panaro, M. D. Giorgi, L. Dominici, D. Ballarini, A. I. Fernández-Domínguez, V. Tasco, M. Cuscunà, A. Passaseo, C. Ciracì, G. Gigli, and D. Sanvitto, ACS Nano **10**, 11360 (2016).
22. Y.-X. Zhang and K. Mølmer, Phys. Rev. Lett. **125**, 253601 (2020).
23. M. A. K. Othman, F. Yazdi, A. Figotin, and F. Capolino, Phys. Rev. B **93**, 024301 (2016).
24. A. F. Cihan, A. G. Curto, S. Raza, P. G. Kik, and M. L. Brongersma, Nat. Photon. **12**, 284 (2018).

FULL REFERENCES

1. A. I. Kuznetsov, A. E. Miroshnichenko, M. L. Brongersma, Y. S. Kivshar, and B. Luk'yanchuk, "Optically resonant dielectric nanostructures," Science **354**, aag2472 (2016).
2. A. B. Evlyukhin, C. Reinhardt, A. Seidel, B. S. Luk'yanchuk, and B. N. Chichkov, "Optical response features of si-nanoparticle arrays," Phys. Rev. B **82**, 045404 (2010).
3. V. E. Babicheva and A. B. Evlyukhin, "Resonant lattice kerker effect in metasurfaces with electric and magnetic optical responses," Laser Photonics Rev. **11**, 1700132 (2017).
4. G. Grinblat, Y. Li, M. P. Nielsen, R. F. Oulton, and S. A. Maier, "Enhanced third harmonic generation in single germanium nanodisks excited at the anapole mode," Nano Lett. **16**, 4635–4640 (2016).
5. M. V. Rybin, K. L. Koshelev, Z. F. Sadrieva, K. B. Samusev, A. A. Bogdanov, M. F. Limonov, and Y. S. Kivshar, "High-q supercavity modes in subwavelength dielectric resonators," Phys. Rev. Lett. **119**, 243901 (2017).
6. K. Koshelev, S. Kruk, E. Melik-Gaykazyan, J.-H. Choi, A. Bogdanov, H.-G. Park, and Y. Kivshar, "Subwavelength dielectric resonators for nonlinear nanophotonics," Science **367**, 288–292 (2020).
7. V. Rutckaia, F. Heyroth, A. Novikov, M. Shaleev, M. Petrov, and J. Schilling, "Quantum dot emission driven by mie resonances in silicon nanostructures," Nano Lett. **17**, 6886–6892 (2017).
8. X. Ma, A. R. James, N. F. Hartmann, J. K. Baldwin, J. Dominguez, M. B. Sinclair, T. S. Luk, O. Wolf, S. Liu, S. K. Doorn, H. Htoon, and I. Brener, "Solitary oxygen dopant emission from carbon nanotubes modified by dielectric metasurfaces," ACS Nano **11**, 6431–6439 (2017).
9. A. García-Etxarri, R. Gómez-Medina, L. S. Froufe-Pérez, C. López, L. Chantada, F. Scheffold, J. Aizpurua, M. Nieto-Vesperinas, and J. J. Sáenz, "Strong magnetic response of submicron silicon particles in the infrared," Opt. Exp. **19**, 4815–4826 (2011).
10. H. Qiao, B. Guan, T. Böcking, M. Gal, J. J. Gooding, and P. J. Reece, "Optical properties of ii-vi colloidal quantum dot doped porous silicon microcavities," Appl. Phys. Lett. **96**, 161106 (2010).
11. S. Kim, J. E. Fröch, J. Christian, M. Straw, J. Bishop, D. Totonjian, K. Watanabe, T. Taniguchi, M. Toth, and I. Aharonovich, "Photonic crystal cavities from hexagonal boron nitride," Nat. Commun. **9**, 2623 (2018).
12. X. Ma, N. F. Hartmann, J. K. S. Baldwin, S. K. Doorn, and H. Htoon, "Room-temperature single-photon generation from solitary dopants of carbon nanotubes," Nat. Nanotechnol. **10**, 671–675 (2015).
13. K.-H. Kim and W.-S. Rim, "Anapole resonances facilitated by high-index contrast between substrate and dielectric nanodisk enhance vacuum ultraviolet generation," ACS Photon. **5**, 4769–4775 (2018).
14. J. Zhou, A. Panday, Y. Xu, X. Chen, L. Chen, C. Ji, and L. J. Guo, "Visualizing mie resonances in low-index dielectric nanoparticles," Phys. Rev. Lett. **120**, 253902 (2018).
15. C. W. Hsu, B. Zhen, A. D. Stone, J. D. Joannopoulos, and M. Soljačić, "Bound states in the continuum," Nat. Rev. Mater. **1**, 16048 (2016).
16. F. Monticone, H. M. Doeleman, W. D. Hollander, A. F. Koenderink, and A. Alù, "Trapping light in plain sight: Embedded photonic eigenstates in zero-index metamaterials," Laser Photonics Rev. **12**, 1700220 (2018).
17. S. T. Ha, Y. H. Fu, N. K. Emani, Z. Pan, R. M. Bakker, R. Paniagua-Domínguez, and A. I. Kuznetsov, "Directional lasing in resonant semiconductor nanoantenna arrays," Nat. Nanotechnol. **13**, 1042–1047 (2018).
18. S. Ayas, A. E. Topal, A. Cupallari, H. Guner, G. Bakan, and A. Dana, "Exploiting native al2o3 for multspectral aluminum plasmonics," ACS Photonics **1**, 1313–1321 (2014).
19. Y. Shen, V. Rinnerbauer, I. Wang, V. Stelmakh, J. D. Joannopoulos, and M. Soljačić, "Structural colors from fano resonances," ACS Photon. **2**, 24–32 (2015).
20. C. S. Kim, A. M. Satanin, Y. S. Joe, and R. M. Cosby, "Resonant tunneling in a quantum waveguide: Effect of a finite-size attractive impurity," Phys. Rev. B **60**, 10962 (1999).
21. F. Todisco, M. Esposito, S. Panaro, M. D. Giorgi, L. Dominici, D. Ballarini, A. I. Fernández-Domínguez, V. Tasco, M. Cuscunà, A. Passaseo, C. Ciracì, G. Gigli, and D. Sanvitto, "Toward cavity quantum electrodynamics with hybrid photon gap-plasmon states," ACS Nano **10**, 11360–11368 (2016).
22. Y.-X. Zhang and K. Mølmer, "Subradiant emission from regular atomic arrays: Universal scaling of decay rates from the generalized bloch theorem," Phys. Rev. Lett. **125**, 253601 (2020).
23. M. A. K. Othman, F. Yazdi, A. Figotin, and F. Capolino, "Giant gain enhancement in photonic crystals with a degenerate band edge," Phys. Rev. B **93**, 024301 (2016).
24. A. F. Cihan, A. G. Curto, S. Raza, P. G. Kik, and M. L. Brongersma, "Silicon mie resonators for highly directional light emission from monolayer mos2," Nat. Photon. **12**, 284–290 (2018).